Xu *et al. Earth, Planets and Space (2019) 71:43*
https://doi.org/10.1186/s40623-019-1023-9

Earth, Planets and Space

FULL PAPER Open Access

A large scale of apparent sudden movements in Japan detected by high-rate GPS after the 2011 Tohoku Mw9.0 earthquake: Physical signals or unidentified artifacts?

Peiliang Xu[1*], Yuanming Shu[2], Jingnan Liu[3], Takuya Nishimura[1], Yun Shi[4] and Jeffrey T. Freymueller[5]

Abstract

A moment magnitude Mw9.0 earthquake hit northeastern Japan at 14:46:18 (Japan Standard Time), March 11, 2011. We have obtained 1 s precise point positioning solutions for 1198 GEONET stations. Although GPS position time series have been routinely investigated and used as waveforms for dynamic inversion of earthquakes, we focus on exploring the spatial displacement features of GEONET stations for this earthquake. A movie inspection of high-rate GPS waveforms leads us to find that 76.21% of the GEONET stations in the Japanese islands subsided suddenly within 1 s between 14:59:45 and 14:59:46, Japan local time, with an average displacement of − 2.43, 2.83 and − 4.75 mm in the east, north and vertical components, respectively, about 15 min after the 2011 Tohoku earthquake. We have performed different types of independent tests, namely measurement error analysis, processing the GEONET data with a different software system, a statistical hypothesis testing under a simple assumption of sign distributions, the test computation of the displacement field outside of the Japanese islands and an independent test with the Japanese strong motion borehole network KiK-net, to see whether these sudden movements actually occurred. The first four independent tests are passed almost without any doubt, and the direction of the average sudden displacements is roughly consistent tectonically with the direction of subduction of the Pacific plate. Because there are only 78 KiK-net borehole stations available for an independent seismic test, the KiK-net results are marginally consistent with those of GEONET. In the daily seismological and geophysical practice, one may then conclude that the sudden movement within the second is real after passing these five independent tests. However, a further epoch-by-epoch check pinpoints a few more seconds with even a higher probability of sudden displacement from the 20-min three-component high-rate GPS waveforms after the main shock, or more precisely, the seconds between 14:59:04 and 14:59:05, 15:01:04 and 15:01:05, and 15:03:39 and 15:03:40 with 80.80, 84.14 and 85.89% of the GEONET stations simultaneously moving upward, southward and westward, respectively. Although these probabilities are very high, it may hardly be imagined that a large scale of sudden movements could occur repeatedly between 14:59:04 and 15:03:40. The high-rate GPS results imply that some detected sudden movements after the earthquake could be unidentified artifacts of GPS data processing, though we cannot rule out the possibility that the detected sudden movements in Japan after the 2011 Tohoku Mw9.0 earthquake are real physical signals.

Keywords: High-rate GNSS, Precise point positioning (PPP), Spatial pattern of deformation, Tohoku Mw9.0 earthquake

*Correspondence: pxu@rcep.dpri.kyoto-u.ac.jp
[1] Disaster Prevention Research Institute, Kyoto University, Uji, Kyoto 611-0011, Japan
Full list of author information is available at the end of the article

Introduction

Geodetic deformation measurements have played an important role in earth sciences and disaster prevention/reduction for years. They are uniquely fundamental to understanding the interseismic, coseismic and post-seismic deformation process of the earthquake cycle and earthquake mechanics (see e.g., Reid 1910; Whitten and Claire 1961; Prescott et al. 1989; Blewitt et al. 1993; Segall 1997; Thatcher et al. 1999). From two geodetic campaigns along the San Andreas fault made in the years 1851–1865 and 1874–1892 before the 1906 California earthquake and one in the years 1906–1907 after the earthquake, Reid (1910) proposed the elastic rebound theory to explain the mechanics of earthquakes, which has since become a landmark theory in seismology and earthquake engineering (Segall 1997; Dieterich 1974). When combining Reid's elastic rebound theory with geodetic measurements, particularly the measurements close to the hypocenter area, one can invert for static rupture models on the fault plane to further understand the physics of earthquakes (Thatcher et al. 1997; Simons et al. 2011; Iinuma et al. 2012). Precise seafloor geodetic displacement measurements have been shown to significantly improve to estimate the static slip distributions for the 2011 Tohoku Mw9.0 earthquake (Sato et al. 2011; Iinuma et al. 2012). Geodetic deformation measurements are used to compute coseismic strain changes due to earthquakes (Whitten and Claire 1961; Frank 1966; Clarke et al. 1998) and to evaluate strain accumulation over time to interpret the process of strain energy accumulation, which may provide clues for earthquake prediction (Fialko 2006). Space geodesy is also an indispensable component of earthquake early warning systems and real-time tsunami monitoring systems.

Japan is a tectonically very active area surrounded by plate margins, subduction zones, trenches and troughs and island arcs, since the oceanic Pacific and Philippine plates, the continental Eurasian plate and the North American plate all meet within the Japanese islands. As a result, Japan is full of high, and sometimes, even catastrophic risks from earthquakes and volcanoes. With strong support from the government and attributed to great effort by Japanese scientists, the Japanese islands are excellently equipped with continuous monitoring infrastructure, with the strong motion monitoring networks "KNET/KiK-net" and the continuous GPS monitoring network "GEONET" as two of the outstanding examples. Thus, Japan may be said to be one of the best natural fields for earthquake experiments in the world.

A moment magnitude Mw9.0 mega-earthquake, called the 2011 Tohoku earthquake, suddenly hit the northeastern Japan at 14:46:18 (Japan Standard Time, according to Japan Meteorological Agency), March 11, 2011 (http://www.jma.go.jp/jma/en/2011/Earthquake/Informationon2011Earthquake.html; Lay and Kanamori 2011). This subduction zone mega-earthquake ruptured an area of about 500 km by 200–300 km (Lay and Kanamori 2011; Simons et al. 2011; Iinuma et al. 2012), with a maximum slip of about 50–60 m, and generated a tragic tsunami along the northeastern coast of Japan, with a maximum run-up height of 40.5 m. The earthquake was well recorded by almost all the earthquake monitoring networks in Japan. Nevertheless, it clipped many seismometers in the northeastern part of Japan. Since seismometers are actually a simplified type of inertial measurement unit without measuring attitudes, seismic data collected at different instants close to the epicenter during a large earthquake are recorded in an instantly different, constantly changing body frame due to rotations and tilts, in addition to saturation, instrumental drifts and clipping, and some data can become unusable (Graizer 2010).

High-rate GNSS has been a hot research topic recently and found a lot of applications in earth sciences and civil engineering (see e.g., Kato et al. 2000; Larson et al. 2003; Larson 2009; Smalley 2009; Grapenthin and Freymueller 2011; Branzanti et al. 2013; Moschas and Stiros 2015; Xu et al. 2013, 2019). A number of methods have been proposed to ensure high precision high-rate GNSS waveform and displacement measurements. Important methodological advances include the invention and application of sidereal and spatiotemporal filters (see e.g., Wdowinski et al. 1997; Choi 2004; Dong et al. 2006; Ragheb et al. 2006; Larson et al. 2007), which enable removal of the effects of multipath and common mode GNSS errors, and precisely reconstruct high-rate GNSS waveforms and displacements. For more information on GNSS seismology, the reader is referred to the review paper by Larson (2009).

Almost all works on high-rate GNSS are focused on precise measurement of temporal waveforms and displacements. In this paper, we will primarily study the spatial variations of coordinates of GNSS stations within very short periods of time, 1 s in our case. We have processed 1 Hz GPS data from 1198 GEONET stations and obtained 1 s precise point positioning (PPP) time series of positions for these stations. A movie of these high-rate PPP waveforms leads us to find that 76.21% of the GEONET stations in the Japanese islands consistently subside suddenly within 1 s between 14:59:45 and 14:59:46.

The major purposes of this paper are twofold: (i) to describe how such a large scale of apparent sudden movements in Japan are identified/detected; and (ii) to make a thorough effort to test whether these apparent

phenomena are physical signals or unidentified artifacts by examining any possible effect of GPS errors, checking the IGS stations outside Japan, processing the GEONET data with a different software system, performing statistical hypothesis testings and further carrying out the independent tests with GEONET and KiK-net data and finally checking epoch-wise PPP waveforms. In what follows, we will describe how the apparent phenomenon of sudden movements is identified/detected and how all the independent tests are carried out to test whether the detected sudden movements are physical signals or artifacts.

Sketch of independent tests

To examine whether the detected large-scale sudden movement after the earthquake is a real physical signal or an artifact, we have come up with six independent tests. The first test is to examine GPS measurement error sources and to confirm that they can either have no or negligible effect on the detected sudden movement within 1 s. The second independent test is to check whether the GEONET displacement pattern over the Japanese islands is consistent with similar sudden movements in the countries surrounding Japan by using the same software system. Both the sudden displacement patterns obtained by processing the high-rate GEONET and IGS GPS data in and outside the Japanese islands are basically fully consistent with each other. As the third independent test, we process the GEONET data with a different (well-known) software system. The displacement results of the GEONET stations from both software systems are consistent as well. Thus, the first three tests are passed successfully. As the fourth independent test, we assume that any GEONET station after the earthquake moves up or down with the same probability at any moment, which is equivalent to making the assumption that such a movement is purely attributed to white noise. This independent test is also passed with large statistical confidence, implying that Japan was subject to a large scale of sudden movement within 1 s about 13.5 min after the 2011 Tohoku earthquake with a large probability.

In addition to GEONET GPS data, the fifth thorough independent test has been carried out to examine the results between 14:59:45 and 14:59:46 with the borehole KiK-net strong motion data. Since the KiK-net stations are only triggered to start recordings of data, we have only a total of 78 borehole KiK-net stations available for this independent test. The KiK-net displacement results are marginally consistent with the detected sudden movement by GEONET. But at least, this fifth independent test with the borehole KiK-net strong motion data can be said to pass marginally. Nevertheless, since strong motion seismographs are well known to have serious problems in integrated displacements due to tilting and baseline shifts and since the number of available borehole KiK-net stations is extremely small, we cannot firmly conclude that the seismic KiK-net is definitely in favor of the detected movement by GEONET.

All reasonable independent tests that geoscientist may think of with both GPS and KiK-net data and in terms of statistical hypothesis testings seem to fully support the phenomenon of sudden movement within 1 s after the earthquake as a real physical signal. As a final independent test, we have checked whether the same phenomenon occurs at other epochs. We have written a computer code to screen the epoch-wise high-rate GPS PPP waveforms of all the GEONET stations. As a result, the computer code pinpoints a few more seconds with even a higher probability from the 20-min three-component high-rate GPS waveforms after the main shock, notably, the seconds between 14:59:04 and 14:59:05, 15:01:04 and 15:01:05, and 15:03:39 and 15:03:40 with 80.80, 84.14 and 85.89% of the 1198 GEONET stations simultaneously moving upward, southward and westward, respectively. From the physical point of view, it seems hard to believe that a mega-earthquake could trigger several sudden movements of large scale within 20 min, though we cannot completely exclude such a possibility either. On the other hand, as GPS experts, both theoretically and/or in practical GPS data processing, we suspect that the detected movements likely are artifacts rather than real physical signals, even though the high-rate PPP waveforms show that as many as 85.89% of 1198 GEONET stations move along one direction within 1 s.

GPS data, data processing methods and results

Displacements from the 2011 Tohoku earthquake were measured on almost all GEONET stations. The GEONET GPS data have been used to determine the displacement waveforms and coseismic fields for inverting rupture models of the 2011 Tohoku earthquake (Simons et al. 2011; Iinuma et al. 2012). For this research, we received, in total, the GPS data of 1221 GEONET stations at the sampling rate of 1 Hz on this mega-earthquake from the Geospatial Information Authority (GSI) of Japan via the Japan Association of Surveyors. Larson et al. (2003) applied kinematic relative positioning method (Larson 2011, private email communication on April 30, 2011) to process the 1 Hz GPS data for the 2002 Denali fault Mw7.9 earthquake and successfully showed that seismic surface waves can be correctly reconstructed from high-rate GPS measurements. For mega-earthquakes like the 2011 Tohoku earthquake, we cannot expect a fixed reference station in Japan, which can be assumed not to move during the earthquake. As a result, we have processed the 1 s sampling GPS data for 1221 GEONET stations by using the GNSS PPP function of the Wuhan University

software package PANDA (*P*osition *A*nd *N*avigation system *D*ata *A*nalysis) (Liu and Ge 2003), since GNSS PPP does not require any reference station; individual stations are positioned relative to the global network used to determine the orbits and clocks. The position time series of seventeen stations are too short to be useful in this work, and six more stations are too noisy with a very large variation, with two stations located in the Kanto area and four in the Tohoku area, respectively. The final number of the GEONET stations used for this report is 1198.

GNSS positioning has almost always been based on two types of GNSS observables, namely pseudoranges and carrier phases. The linearized observational equations of a pseudorange and a carrier phase observable between a satellite and a receiver can be written as follows:

$$\begin{aligned} P_r^s &= \rho(\mathbf{x}_r, \mathbf{x}^s) + I_r^s + T_r^s + c(\delta t_r - \delta t^s) \\ &\quad + \delta b_r^p - \delta b_s^p + \epsilon_{mp} + \epsilon_p, \end{aligned} \tag{1a}$$

$$\begin{aligned} L_r^s &= \rho(\mathbf{x}_r, \mathbf{x}^s) - I_r^s + T_r^s + c(\delta t_r - \delta t^s) \\ &\quad + \lambda N + \delta b_r^l - \delta b_s^l + \epsilon_{ml} + \epsilon_l, \end{aligned} \tag{1b}$$

where P_r^s and L_r^s are, respectively, the code and phase observables between satellite s and receiver r, $\rho(\cdot,\cdot)$ is the geometric distance between this pair of satellite and receiver. $\mathbf{x}_r$ and $\mathbf{x}^s$ stand for the positions of the receiver and the satellite, respectively. I_r^s and T_r^s are the ionospheric and tropospheric delays. δt_r, δt^s, δb_r^p, δb_s^p, δb_r^l and δb_s^l are the clock errors and the hardware code and phase biases of the receiver and the satellite, respectively. λ is the wavelength of the carrier wave, and N is the unknown integer of full cycle. ϵ_{mp} and ϵ_{ml} are the multipath errors of the code and carrier phase observables, respectively, which are frequency-dependent. ϵ_p and ϵ_l are the measurement noises of the code and carrier phase observables P_r^s and L_r^s, respectively. The observational Eq. (1) symbolically applies to all frequencies and GNSS systems. We may note that the code biases δb_r^p and δb_s^p of (1a) can be corrected with the IGS products, and as a result, can be merged into the pseudorange P_r^s. The carrier phase observable L_r^s of (1b) is supposed to include the satellite/receiver antenna PCO/PCV and wind-up corrections.

To attain the highest possible GNSS positioning accuracy, we have to either eliminate or correct all the systematic error terms in the observational Eq. (1). The former has been achieved in geodesy since the inception of GPS by applying the double difference operator to both code and phase measurements, if a baseline is sufficiently short. The latter has led to the innovative development of PPP by Zumberge et al. (1997). Since there is no fixed/reference station during a mega-earthquake like this 2011 Tohoku Mw9.0 earthquake, GNSS PPP processing is preferred over precise GNSS relative positioning for this research.

For conciseness of notation, in what follows, we will ignore superscripts/subscripts s and r for satellites and receivers. As in the case of other most widely used software systems such as GAMIT and GIPSY-OASIS, PANDA PPP uses ionospheric-free combinations of dual frequency P-code and carrier phase observables:

$$P_3 = \frac{f_1^2}{f_1^2 - f_2^2} P_1 - \frac{f_2^2}{f_1^2 - f_2^2} P_2, \tag{2a}$$

$$L_3 = \frac{f_1^2}{f_1^2 - f_2^2} L_1 - \frac{f_2^2}{f_1^2 - f_2^2} L_2, \tag{2b}$$

(see e.g., King et al. 1985; Brunner and Gu 1991; Bassiri and Hajj 1993), where $f_i (i = 1, 2)$ are the L1 and L2 frequencies, and $L_i (i = 1, 2)$ and $P_i (i = 1, 2)$ are the raw carrier phase and code observations in the L1 and L2 frequencies, respectively. Since the GEONET stations are all equipped with choke rings to eliminate or mitigate multipath errors, both ϵ_{mp} and ϵ_{ml} can be omitted from (1). On the other hand, receiver and satellite phase biases cannot be separated from the ambiguity unknowns. As a result, GNSS PPP data processing is based on linearizing the ionospheric-free P-code and carrier phase observables (2):

$$\delta P_3^{kt} = \boldsymbol{a}_{kt} \Delta \boldsymbol{x}_t + \Delta e_t + \Delta T_k + \epsilon_{p3}^{kt}, \tag{3a}$$

$$\delta L_3^{kt} = \boldsymbol{a}_{kt} \Delta \boldsymbol{x}_t + \Delta e_t + \Delta T_k + \lambda_{if} N_{if}^k + \epsilon_{l3}^{kt}, \tag{3b}$$

to estimate four types of unknown parameters from ionospheric-free pseudoranges and carrier phase observables, namely the unknown coordinates of a station, the receiver clock error, the residual tropospheric delays and the non-integer ambiguities, where δP_3^{kt} and δL_3^{kt} are, respectively, the ionosphere-free code and phase observables after subtracting the corresponding approximate range between the kth satellite and the receiver. All model corrections have been fully taken into account in δP_3^{kt} and δL_3^{kt}, except for their residual errors. The superscript and subscript k stands for the kth satellite, $\boldsymbol{a}_{kt}$ is the given row vector of the linearization coefficients, $\Delta \boldsymbol{x}_t$ is the vector of the coordinate corrections of the receiver at the epoch t in the local reference frame with the axes pointing to east, north and upward, Δe_t is the receiver clock range correction to be estimated at each epoch, ΔT_k is the correction to tropospheric path delay to be estimated, λ_{if} is the wavelength of the ionosphere-free frequency, N_{if}^k is a non-integer ionosphere-free ambiguity unknown, and ϵ_{p3}^{kt} and ϵ_{l3}^{kt} represent the (systematic and random) residual errors of the ionosphere-free observables. In this study, *a*

priori values of standard deviations for ionosphere-free phase and code observables are set to 3 mm and 30 cm, respectively. For more methodological details about PPP, the reader may refer to Kouba (2009) (see also Kouba and Héroux 2001).

When PANDA is used to process GPS data in PPP mode, it generally takes about 20–30 min for the floating ambiguities to converge. Actually, to be more careful and to make sure the correctness of our processing results, we have continuously processed almost 4 h of static GPS data before starting to compute the converged PPP solutions or waveforms for the 2011 Tohoku Mw9.0 earthquake. Although the code observables are important to help speed up the convergence of ambiguity resolution, after the convergence of the floating ambiguities, the precision of PPP coordinate solutions is basically solely determined by carrier phase observables. PANDA further implements the second-order ionosphere corrections. Since the tropospheric parameters are generally estimated for a session of 2 h, and since the converged floating ambiguities can be treated as part of phase observables, we can then use the simplified observation Eq. (3b), namely

$$\delta y_3^{kt} = \boldsymbol{a}_{kt}\Delta\boldsymbol{x}_t + \Delta e_t + \epsilon_{l3}^{kt}, \tag{4}$$

to compute the precise GPS PPP solutions of coordinates within each session, where $\delta y_3^{kt} = \delta L_3^{kt} - \Delta T_k - \lambda_{if} N_{if}^k$. We should like to note that in order to avoid any potential effect of discontinuity of the estimated tropospheric parameters at the end points of the 2 h session, we have carefully set the 2 h session of tropospheric corrections to roughly cover the earthquake at its central part of the session. Thus, tropospheric corrections are smoothly continuous without any dislocation/discontinuity. Although ϵ_{l3}^{kt} can affect precise PPP positioning up to a few centimeters over a time period of a few tens of minutes to years, experiments have clearly shown that precise PPP positioning can reach mm level of accuracy for changes in displacements over a short period of time (Xu et al. 2013; Shu et al. 2017).

The weighting function used in PANDA PPP is elevation dependent and given by

$$w(A_\mathrm{e}) = \begin{cases} 1, & \text{if } A_\mathrm{e} > 30^\circ \\ 2\sin(A_e), & \text{if } A_\mathrm{e} \le 30^\circ \end{cases} \tag{5}$$

where A_e is the elevation angle of a GPS satellite. In post-processing mode, we use the International GNSS Service precise orbits and 5-s precise clock products from the Center for Orbit Determination in Europe (CODE) to compute the position waveforms of the GEONET stations. PANDA follows the IERS conventions 2003 to correct tidal effects and antenna phase center variations and uses the Saastamoinen model with the global mapping function of Boehm et al. (2006) to correct tropospheric delays.

Based on the 1 Hz PPP time series of positions obtained for these 1198 GEONET stations, we first inspected the PPP waveforms and identified a sudden displacement pattern over the whole GEONET network at a specific epoch soon after the 2011 Tohoku earthquake, namely the second between 14:59:45 and 14:59:46. We wrote a computer code to check whether this phenomenon occurs at other epochs. The computer code found a few more seconds at 14:59:04, 15:01:04 and 15:03:39 with even a higher probability from the 20-min three-component high-rate GPS waveforms after the main shock, showing that 80.80, 84.14 and 85.89% of the GEONET stations simultaneously move along the same directions, respectively. In this paper, we will carry out a detailed analysis of the first inspected epoch to demonstrate how an artifact may be reported as a real physical signal, even though we cannot be certain that the apparent sudden movements detected by high-rate GPS PPP are indeed not physical.

Figure 1 shows the displacements between these two epochs for the GEONET network in the east, north and vertical directions. For a better visual effect, we only show the stations that subside in Fig. 1a. The corresponding displacement vectors are also shown in Fig. 2. Among the 1198 GEONET stations, 913 stations, i.e., 76.21% of the stations, have negative vertical displacements. Among these stations, the maximum and mean values of sudden vertical movements are −39.08 mm and −4.75 mm, respectively. Listed in the appendix of electronic materials are the three-component displacements between the epochs of 14:59:45 and 14:59:46 for all the GEONET stations (Additional file 1: Table S1).

We have also used 30 min of the position time series before the earthquake to evaluate the standard deviations of displacements between two consecutive epochs. To avoid the effect of any spikes in coordinates in the time series, we use the sign-constrained robust least squares method (Xu 2005) to estimate the standard deviations of the position series. The robust trimmed mean estimates of the standard deviations for the coordinate differences between two consecutive epochs from the 1198 stations are 2.02 mm, 2.17 mm and 5.00 mm for the east, north and vertical components, respectively, which are consistent with the error evaluation of high-rate GPS PPP solutions (Xu et al. 2013) and further confirmed by a recent theoretical high-rate PPP error analysis (Shu et al. 2017).

Table 1 shows that among the GEONET stations, 66.44% move toward the west direction between 14:59:45 and 14:59:46 (compare panel b of Fig. 1). If we focus on the northeastern area, the percentage basically remains

unchanged, with the mean displacement of −2.43 mm. Since the robust mean standard deviation between two consecutive epochs in the east component of the positioning solutions is about 2.02 mm, the mean displacement is only slightly beyond one standard deviation. However, by treating the signs of displacements for these 1198 stations as Bernoulli statistical experiments, the pattern for 796 out of 1198 stations to move westward within 1 s is clearly significant statistically, as will be confirmed in the next section. In the case of the north component of the displacements, about 66.28% of the stations suddenly move northward (compare panel c of Fig. 1), with the mean displacement of 2.83 mm, which is also only slightly beyond one standard deviation (2.17 mm). Nevertheless, as in the cases of the vertical and eastern components, the pattern of sudden movement toward the north direction is statistically significant. This movement occurred before any of the major M7.0 aftershocks during the 2011 mega-earthquake, because the first aftershock with a magnitude larger than 7.0 occurred at 15:08, about 20 min after the main shock (Huang and Zhao 2013). Although an aftershock of magnitude M6.4 (Huang and Zhao 2013) and likely one more aftershock with a magnitude larger than M6 according to the NIED Web site occurred up to 15:06, an earthquake of magnitude M6 can, at most, produce some local effect, but should not be expected to affect the sudden movement over all the Japanese islands.

First independent tests: measurement errors, IGS stations outside Japan and results from a different software system

Although sidereal and spatiotemporal filters are essential for precise measurement of high-rate GNSS waveforms and displacements, they have no role to play in the case of the variations of coordinates of GNSS stations over such a short period of time. Any common mode errors (CME) and multipath can be reasonably assumed to remain almost constant within 1 s. As a result, their effects within this second remain almost constant as well and are canceled out if we compute the difference of these almost constant effects between two consecutive epochs.

The detected apparent sudden movements cannot be explained by GPS CME over a large area, which are generally of seasonal and secular nature and can be removed by spatiotemporal filtering of GPS daily positions of months to years, with CME sources of environmental and observation technology origins such as unmodeled or mismodeled errors of satellite orbits, reference frame, large-scale atmosphere residual errors, receiver and satellite antenna phase center mismodeling (Wdowinski et al. 1997; Dong et al. 2006). In the timescale of seconds, the effect of all these CME contributions will remain constant and, as a result, will not affect our results of movement over 1 s. Wdowinski et al. (1997) attributed the CME in the vertical component to satellite orbital and reference frame errors. Since both IGS precise satellite orbits and reference frame errors are smooth over hours, at the very least, they should have no effect on the detected vertical sudden movement within 1 s.

To further show that the sudden movements within 1 s reported in Table 1 appear not likely from GNSS error sources of any kinds in our knowledge, we have estimated the effect of each major error source of ϵ_{l3}^{kt} on the PPP-derived displacement within 1 s, under fairly general conditions and/or with model data such as PCO/PCV directly from GEONET. Since no GEONET stations during the 2011 Tohoku Mw9.0 earthquake are used to produce the 5-s CODE precise satellite clock products, we do not expect any potential bias in the precise clock products that might be related to the detected sudden movements. Thus, we only need to investigate the effect of interpolating the precise satellite clock errors. In this case, we assume an instant uncertainty of clocks equivalent to 2 cm in ranging and follow Bock et al. (2009) by assuming a degradation of accuracy loss smaller than 2% from linearly interpolating the 5-s CODE precise clock corrections to compute its effect on PPP within 1 s. The final effects of these major error sources within 1 s are summarized in Table 2. Although the second-order ionospheric corrections (Bassiri and Hajj 1993; Brunner and Gu 1991) have been fully implemented in PANDA, we have still listed the maximum second-order effects of ionosphere on the PPP displacements in Table 2. The second-order effects of ionosphere on the sudden movement within the second of concern for all these 1198 GEONET stations are shown in Fig. 3, with a maximum effect of about 0.008 mm in the vertical direction.

Table 2 clearly shows that the maximum effects on PPP displacements within 1 s are from precise satellite clock errors. All the other residual systematic errors have a much smaller effect on PPP displacements from 1 s to the next. The typical clock errors amount to only about 0.1 mm, or equivalently, about one part in twenty to fifty of the standard deviations between two consecutive epochs. The maximum effect of the instant precise satellite clock uncertainty on the movement within 1 s is in the vertical direction but is only 0.014 mm. The only potential additional sources of bias that we can think of would relate to a sudden deformation of one or more global network station, such as an unmodeled coseismic displacement. However, such an effect is very unlikely in this case because the global solution did not use stations in Japan. Furthermore, we interpolate the clock solutions

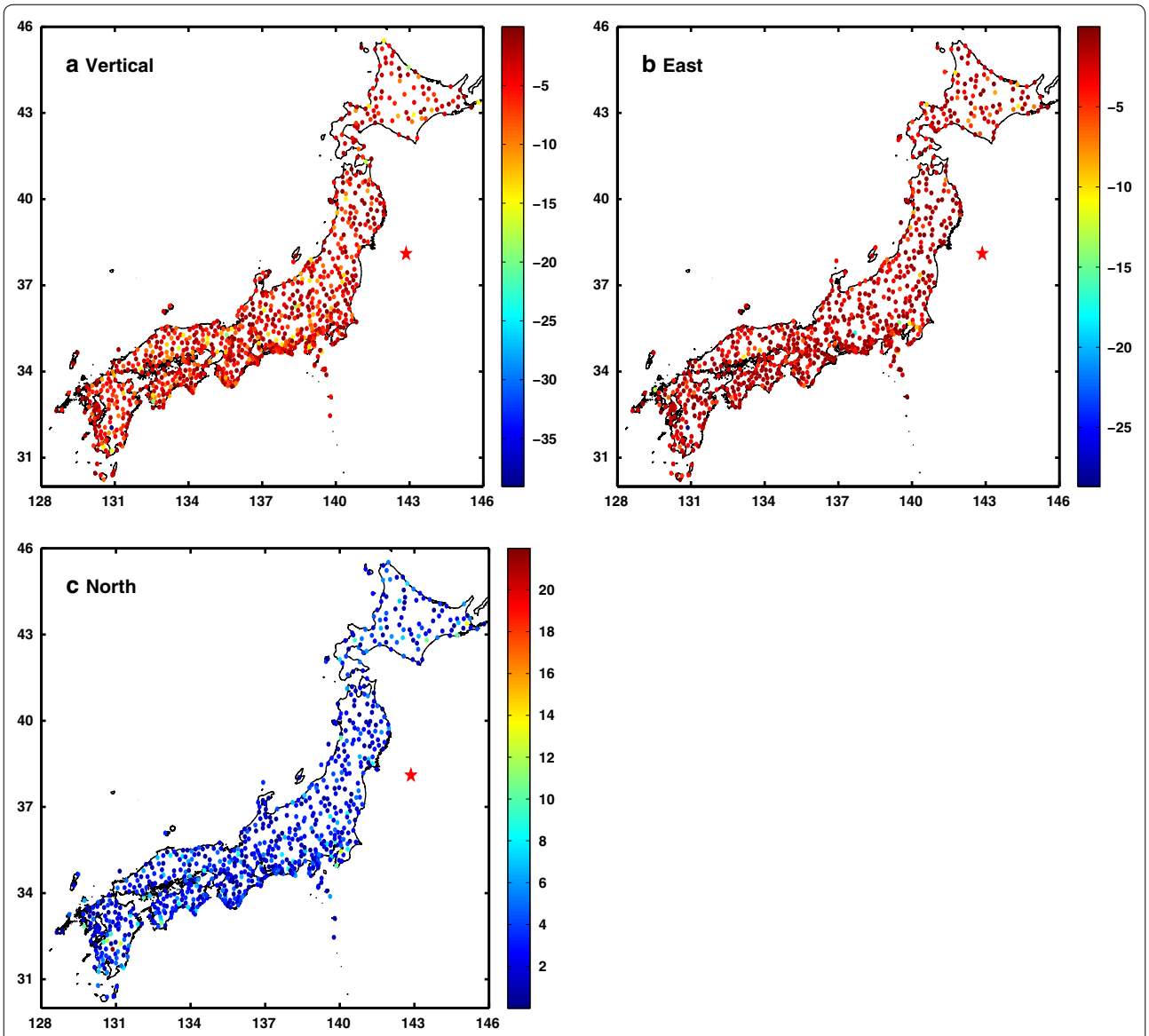

Fig. 1 Three components of sudden displacements (mm) within 1 s between 14:59:45 and 14:59:46 over the GEONET network, with the red star showing the epicenter of the 2011 Tohoku earthquake: panel **a**—the vertical displacements of the GEONET stations that move downward; panels **b** and **c**—the displacements of the GEONET stations that move in the east and north directions

that are provided at 5-s intervals, so any such error would not have an abrupt nature in our solutions.

We have computed PPP solutions for several IGS and other stations to the west of Japan using PANDA, which are shown in Fig. 4. The displacements within 1 s at these stations are listed in Table 3. Although the amplitudes of seismic waveforms at station DAEJ and those along the Chinese border are between 15 and 25 cm and those at the far-field stations like PIMO, YAKT and ULAB are around 10 cm, the movements within the second of our interest range from −6.57 to 0.86 mm in the east component, −0.36 to 5.35 mm in the north component, and −3.13 to 6.63 mm in the up component, respectively. In general, all these stations show a trend to move westward, northward and downward, which is more or less consistent with the trend detected with the GEONET stations on the Japanese islands. Since the CODE clock estimates are not involved with the GEONET stations, we conclude that a bias in the GPS solutions is not a likely explanation for the abrupt displacement.

Additionally, to check and confirm our PPP positioning solutions of the GEONET stations, we have also

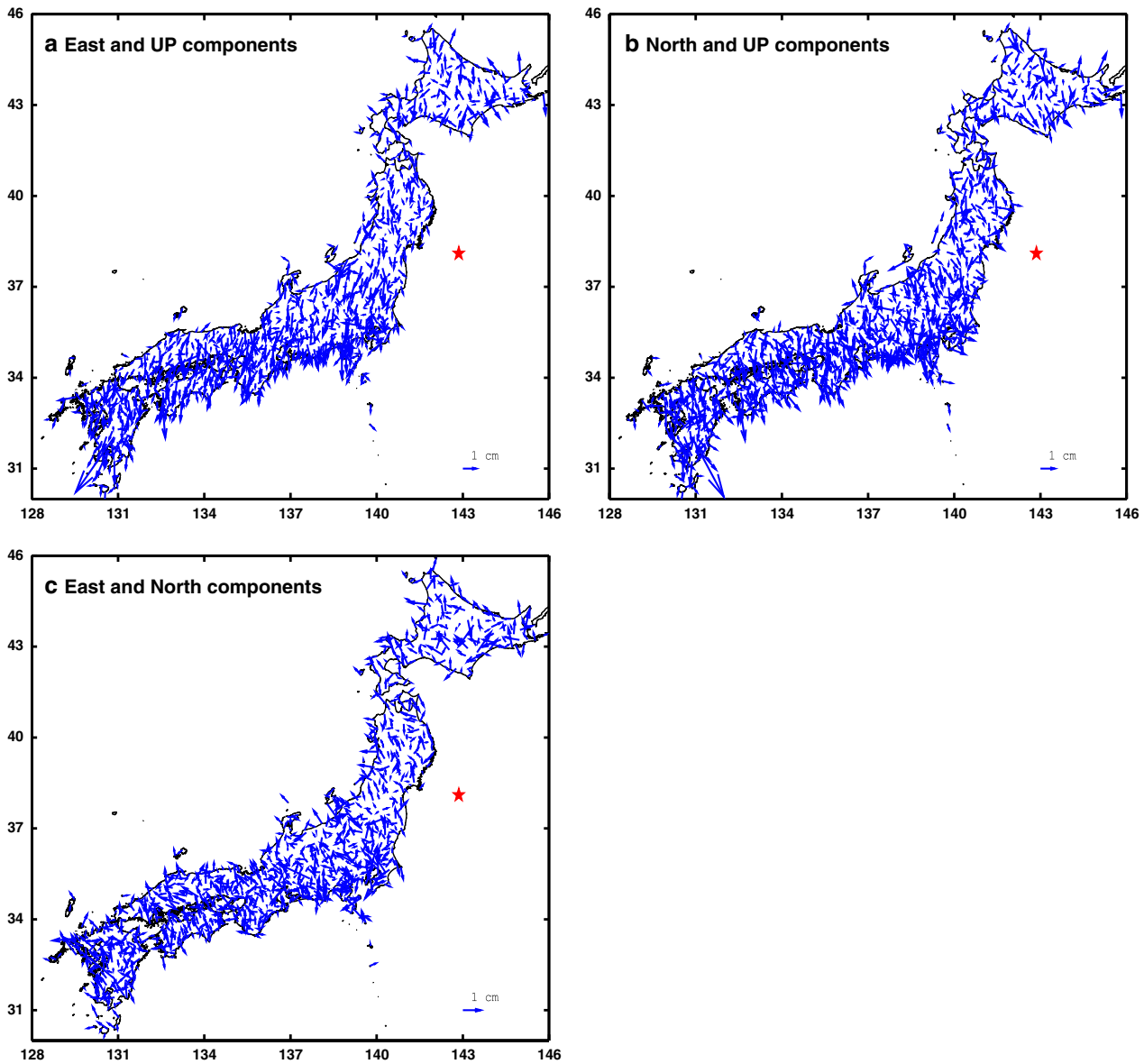

Fig. 2 Sudden displacement vectors (unit length: 1 cm) within 1 s between 14:59:45 and 14:59:46 from all the GEONET stations. The red star stands for the epicenter of the 2011 Tohoku earthquake. Panel **a** shows the sudden displacement vectors of east (horizontal axis) and up (vertical axis) components. The horizontal and vertical axes indicate that the stations basically move westward and downward, respectively. Similarly, panels **b** and **c** show the sudden displacement vectors of north (horizontal axis) and up (vertical axis) components, and east (horizontal axis) and north (vertical axis) components of the GEONET stations, respectively. The vertical axis of the north components in panel **c** indicates that the stations basically move northward

processed the GEONET 1 s sampling GPS data in the PPP mode by using a different GNSS software system, more precisely, GIPSY-OASIS. Both software systems PANDA and GIPSY-OASIS are methodologically similar and start with the same observational model of ionosphere-free phase and code observables. The total number of stations for which both GNSS software systems PANDA and GIPSY-OASIS have successfully processed is 1104. By comparing the PPP results of PANDA with those of GIPSY-OASIS, we have found that on average, 88.38% of these 1104 GEONET stations have shown the same pattern of the displacements. Although 11.62% of the stations show a different direction of displacement, all of these stations have a small displacement, with an absolute mean value of 0.66 mm, 0.90 mm and 1.64 mm for the east, north and vertical components, respectively. In

Table 1 Statistics of the three components of sudden displacements from the 1198 GEONET stations between 14:59:45 and 14:59:46 after the 2011 Tohoku earthquake

Measures	East component	North component	Vertical component
Number of stations	796	794	913
Percentage (GEONET)	66.44	66.28	76.21
Percentage (northeastern)	65.59	69.35	76.88
Mean values (mm)	− 2.43	2.83	− 4.75
Standard deviations (mm)	2.02	2.17	5.00

The first row lists the numbers of stations to move westward, northward and downward, respectively. The next two rows list the percentages of displacements from the whole GEONET network and the northeastern Japan, respectively. The percentages in the vertical component are referred to downward movement. The fourth row lists the mean values of displacements in the east, north and vertical directions. The last row gives the robust adaptive mean values of standard deviations of displacements between two consecutive epochs, as computed from the 30 min of GEONET GPS data before the earthquake

other words, the sudden movements at these stations are well within random errors, and at all other stations, the PANDA and GIPSY solutions are consistent.

The pattern of sudden subsidence may not be random with a high probability

Although other research groups also processed the GEONET GPS data in the PPP mode, they either obtained solutions over a longer interval of time (Simons et al. 2011) or selected a few stations to test the improvement of new PPP methods (Li et al. 2013). Simons et al. (2011) used JPL's GIPSY-OASIS software to estimate kinematic PPP solutions of the GEONET stations at the interval of 5 min, determined the coseismic displacements and estimated a slip distribution model for the 2011 Tohoku earthquake. The 30 s PPP solutions were also made publicly available by the ARIA team at JPL and Caltech (ftp://sideshow.jpl.nasa.gov/pub/JPL_GPS_Timeseries/japan/30sec_sol/) and used to demonstrate the wave motion of the 2011 Tohoku earthquake (Grapenthin and Freymueller 2011). The major purpose of Li et al. (2013) was to test new PPP methods for use in earthquake/tsunami monitoring.

Although the mean value of the vertical movements is within one time of the vertical standard deviation and might be thought to be not significant for each individual station from the statistical point of view, the pattern of such movements over the whole GEONET network is clearly not random. Actually, instead of using the rule of thumb of 2 or 3 times sigma to statistically judge whether a value is significant in terms of its magnitude, it is more appropriate to use statistical sign testing to see whether measurements exhibit a certain pattern or trend. If we assume a simple stochastic model that the vertical component of displacement between 14:59:45 and 14:59:46 for each station is random with mean zero, then the signs "*downward*" and "*upward*" of a random vertical displacement can be equivalently interpreted stochastically as the events of "*success*" and "*failure*" of a random variable, and thus, can be described by using a Bernoulli distribution (Mood et al. 1974), namely

$$P(S) = \begin{cases} p, & \text{if the station moves downward} \\ 1-p, & \text{if the station moves upward} \end{cases} \tag{6}$$

where p stands for the probability that the station moves downward. If the vertical movement of a station is only contaminated by random errors with mean zero, then the probability of moving downward is equal to 0.5, i.e., $p = 0.5$, implying that the station moves equally likely, either upward or downward. If the same experiments are stochastically repeated independently n times, then the corresponding distribution is binomial, namely

$$P(n_s = k) = C_n^k p^k (1-p)^{n-k}, \tag{7}$$

where n_s stands for the number of times that k stations move downward, and C_n^k for the number of combinations, which is the number of possible ways to have k stations moving downward among n stations. If n_s is sufficiently large, say larger than 1000, then the binomial distribution can be approximated by using a normal distribution with mean np and variance $np(1-p)$ (Mood et al. 1974).

To statistically explain the GPS-observed results of vertical movements, we now assume that we repeat the same experiments 1198 times, calculate the probability that k experiments produce the same negative sign (i.e., move downward) and plot it in Fig. 5. The probability for 913 out of 1198 stations to move simultaneously within 1 s is very small. If we focus on the northeastern area of Japan, then the percentage of such stations slightly increases from 76.21 to 76.88%. Thus, we may conclude that the pattern of the GPS-observed sudden vertical movements over (the GEONET of) Japan after the 2011 Tohoku Mw9.0 earthquake is not random with a high probability.

An independent test of the sudden motion patterns with the strong motion data from KiK-net

As an important infrastructure of large earthquake observation, two major strong motion networks have been constructed after the 1995 Hyogoken-Nanbu (Kobe) earthquake, namely K-NET with about 1000 stations almost uniformly installed on the surface of the Japanese islands with an average distance of about 20 km and KiK-net with about 700 pairs of stations. The KiK-net stations are more sensitive and also uniformly

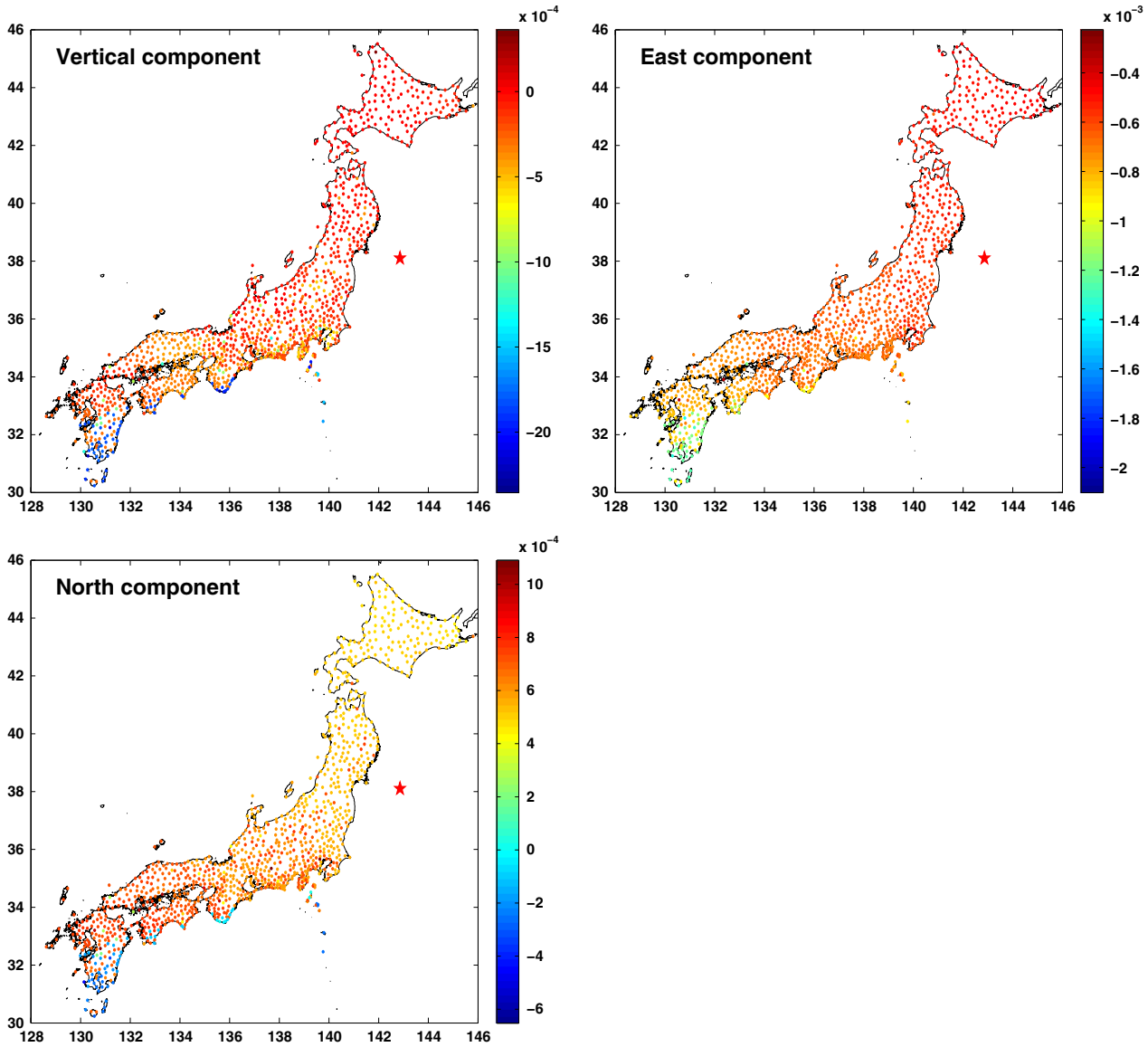

Fig. 3 The second-order effects (units: mm) of ionosphere on the sudden movements of all the GEONET stations within 1 s between 14:59:45 and 14:59:46, corresponding to the vertical, east and north directions, respectively. The red star stands for the epicenter of the 2011 Tohoku earthquake

Table 2 Effects of residual systematic errors on PPP displacements within 1 s (units: 1.0E−3 mm)

Residual errors	Descriptions	Effects on PPP displacements (1 s)		
		East	North	Up
ϵ^i_{so}	Precise satellite orbit error	− 0.13	− 0.19	0.34
ϵ^i_{st}	Precise satellite clock error	− 137.94	− 65.22	− 128.83
ϵ^i_{tr}	Residual errors of tropospheric delay	− 0.41	− 0.14	− 4.91
ϵ^i_{io}	Second-order ionospheric delay	− 4.92	2.44	8.27
ϵ^i_{pc}	Residual satellite/receiver PCO/PCV errors	0.04	0.06	0.09
ϵ^i_{mp}	Multipath errors	− 0.51	0.18	− 3.48

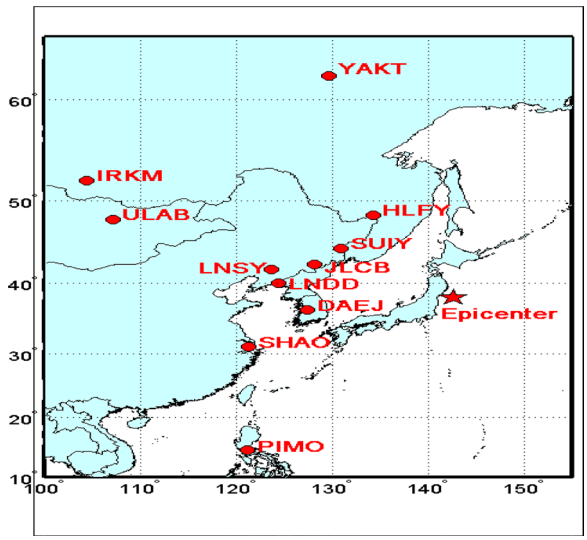

Fig. 4 GNSS stations to the west of Japan

Table 3 PPP displacements (units: mm) within 1 s for the GNSS stations to the west of Japan

Stations	East	North	UP
DAEJ	− 0.48	5.35	0.83
SHAO	− 3.75	1.63	0.79
HLFY	− 0.81	1.70	− 1.38
JLCB	− 1.06	0.82	− 3.13
LNDD	− 2.02	1.13	− 3.06
LNSY	− 6.57	2.23	2.91
SUIY	− 2.10	2.19	− 1.52
IRKM	− 2.36	3.68	6.63
ULAB	− 0.98	− 0.36	− 0.22
YAKT	0.86	3.27	− 1.74
PIMO	− 1.43	1.84	− 3.07

installed in pairs, with one seismograph on the ground surface and the other in a borehole of more than 100 m in depth. The K-NET and KiK-net stations are triggered to start data recording if ground motions satisfy the pre-defined condition of acceleration. For more technical details about these two basic strong motion observation networks in Japan, the reader is referred to Kinoshita (1998), Aoi et al. (2004) and/or directly to the Web site of the National Research Institute for Earth Science and Disaster Prevention (NIED) at http://www.kyoshin.bosai.go.jp/kyoshin/.

Wang et al. (2013) performed a substantially detailed analysis and comparison of the K-NET and KiK-net strong motion and GEONET GPS coseismic displacements during the 2011 Tohoku Mw9.0 earthquake and concluded that the K-NET and KiK-net surface strong motion data cannot be useful for the following two reasons: (i) The coseismic displacements from the K-NET and surface KiK-net data show a large variability, even for the stations close to each other; (ii) these large variations of K-NET/KiK-net-derived coseismic displacements from the corresponding GEONET values are likely attributed to large transient tilting of accelerators and nonlinear baseline shifts and (iii) there are outliers in the strong motion-derived coseismic displacements. When comparing the coseismic displacements from the borehole KiK-net seismograms with those from GEONET, they concluded a root-mean-squared error (rmse) of 0.47 m. After applying an outlier detection and removal strategy to the borehole KiK-net coseismic displacements, the rmse is still as large as about 0.25 m. Since GPS PPP has been repeatedly confirmed to be of cm level of accuracy in the long term and even mm level of accuracy in the short term in the past 20 years or so, the coseismic displacements from the borehole KiK-net after performing all the necessary corrections such as tilting and baseline corrections are in no way comparable with those from GEONET in terms of both accuracy and reliability, even though seismometers have been well known to be more sensitive than GPS.

To further test the reliability and accuracy of seismic waveforms by integrating the borehole KiK-net accelerations, we have selected five borehole KiK-net stations that are the closest to the GEONET stations within a horizontal range of 5.7–24.4 m, as shown in Fig. 6. A direct integration of raw seismographs leads to totally messy and divergent displacement waveforms for these five stations. As a result, we apply three different threshold values of 0.005, 0.01 and 0.05 Hz to high-pass filter the borehole KiK-net accelerations and integrate them to obtain the seismic waveforms of these stations for the main shock and some immediate aftershocks, which are plotted in Fig. 7, together with the PPP waveforms of the corresponding nearby GEONET stations. We can observe from Fig. 7: (i) The seismic waveforms strongly depend on the threshold frequencies; (ii) the seismic waveforms require baseline corrections to be useful, even though criteria for baseline corrections are more or less arbitrary; and (iii) the seismic waveforms can be significantly different from the GEONET PPP waveforms, as can be readily inferred by comparing the waveforms from both GPS and seismograms in Fig. 7 either on the same earthquake (right panel) or different earthquakes (left panel). Actually, without first knowing the independent GPS PPP waveforms, we simply cannot say anything about the reliability and accuracy of seismic waveforms

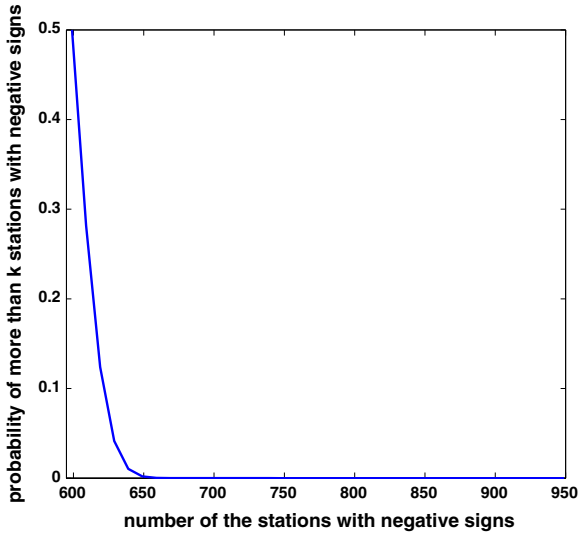

Fig. 5 Probability for *k* vertical displacements to have the negative sign over the whole GEONET network

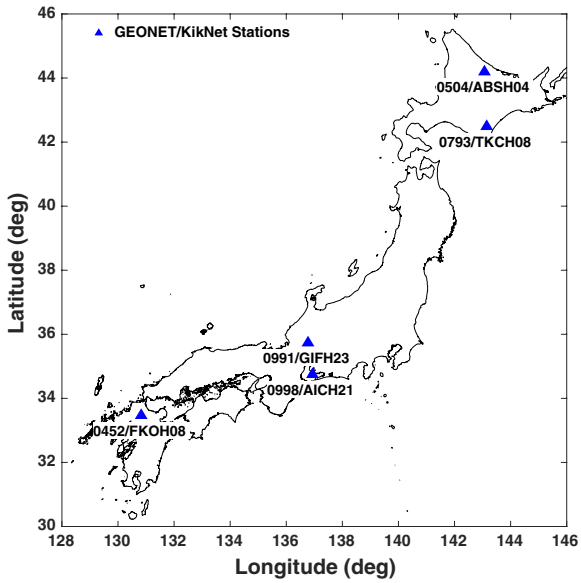

Fig. 6 The five almost collocated KiK-net and GEONET stations, with a horizontal distance of 5.7 m (AICH21, 0998), 7.4 m (GIFH23, 0991), 10.1 m (TKCH08, 0793), 11.4 m (ABSH04, 0504) and 24.4 m (FKOH08, 0452), respectively

at these five borehole KiK-net stations at all. From this point of view, precise high-rate space geodesy should play an even more important role in seismology and disaster mitigation/prevention in the future.

Even with the inherent problems of seismometers in mind, we attempted to make this independent test of the GEONET results of sudden movements with the borehole KiK-net seismograms. According to the web site of NIED, four earthquakes triggered the recordings of KiK-net stations before 15:00, namely earthquakes M9.0 at 14:46, M6.8 at 14:51, M5.8 at 14:54 and M6.4 at 14:58. The aftershocks with a magnitude larger than M6.0 are not consistent with the relocation results of Huang and Zhao (2013), which should not be much of our concern, because any earthquake of magnitude M6 is not expected to affect the whole Japanese islands and beyond. Although the main shock triggered the recordings at 525 KiK-net stations, because the KiK-net seismograms last only for 5 min, we can finally identify a total of 78 borehole KiK-net stations available for this independent test. Since we have no practically objective and operational way to judge which high-pass filter is the best suitable to process the seismograms for a particular earthquake, we will perform the independent test with the high-pass filtered displacement waveforms with a (more or less arbitrary) pre-defined frequency of 0.05 Hz from all these 78 borehole KiK-net stations without any (tilting and/or baseline) corrections over the second. The displacement results are marginally consistent with those of GEONET, or more precisely, with 48, 50 and 45 stations (or equivalently 61.5%, 64.1% and 57.7%) moving along the same east, north and vertical directions as the detected GPS movement. We note that these testing results are similar to those with the original non-filtered displacement waveforms (precisely 59.0%, 48.7% and 60.3%) and with the pre-defined frequency of 0.01 Hz (precisely 57.7%, 62.8% and 52.6%). In the case of 0.005 Hz, the marginal support almost disappears. Without knowing the true and/or GPS waveforms in advance, one would have no practical idea about which seismic waveform result is correct, which further implies the uncertainty, unreliability and even tricky use of seismic waveforms. Because the number of the available borehole KiK-net stations is extremely small, and because of the well-known problems with seismographs, we could not firmly conclude from the borehole KiK-net testings whether the detected sudden movement is definitely real or an unidentified artifact of GPS data processing.

A direct epoch-by-epoch test with GPS PPP waveforms

To check whether the phenomenon of sudden movement between 14:59:45 and 14:59:46 also occurs at other epochs, we wrote a computer code for this purpose, which pinpoints a few more second epochs with even a higher probability from the 20-min three-component high-rate GPS PPP waveforms after the main shock, or more precisely, the seconds between 14:59:04 and 14:59:05, 15:01:04 and 15:01:05, and 15:03:39 and

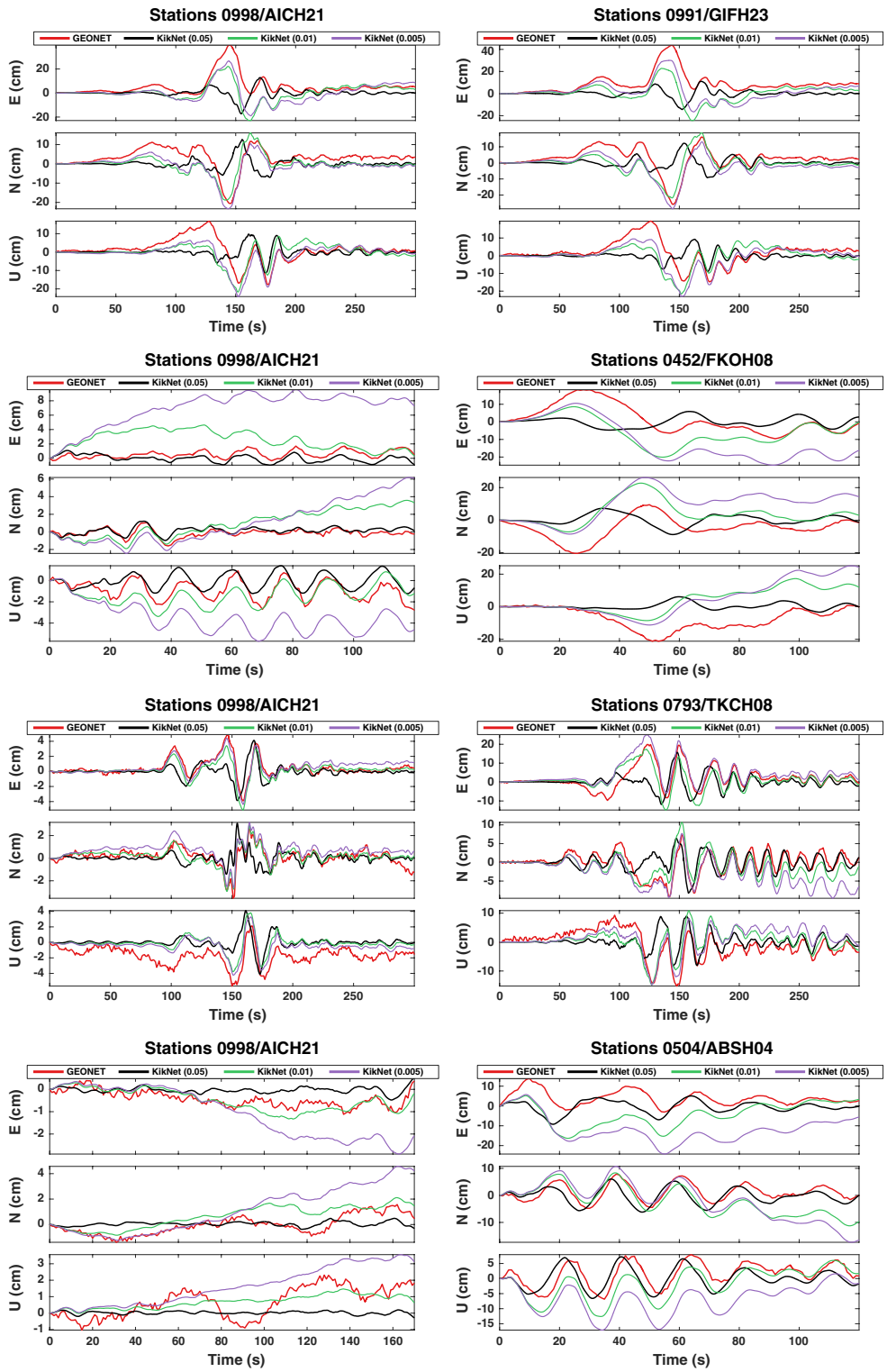

Fig. 7 The seismic waveforms of the KiK-net stations (AICH21, GIFH23, FKOH08, TKCH08 and ABSH04) from high-pass filtering and integrating the borehole KiK-net seismograms with different threshold frequencies (0.005, 0.01 and 0.05 Hz), together with the GPS PPP waveforms of the corresponding closest GEONET stations. The waveforms of the main shock at 14:46 and three immediate aftershocks at 14:51, 15:15 and 15:26 at the KiK-net station AICH21 (almost collocated with the GEONET station 0998) are shown on the left panel. The right panel shows the waveforms of the main shock at the KiK-net stations GIFH23, FKOH08, TKCH08 and ABSH04, almost collocated with the GEONET stations 0991, 0452, 0793 and 0504, respectively

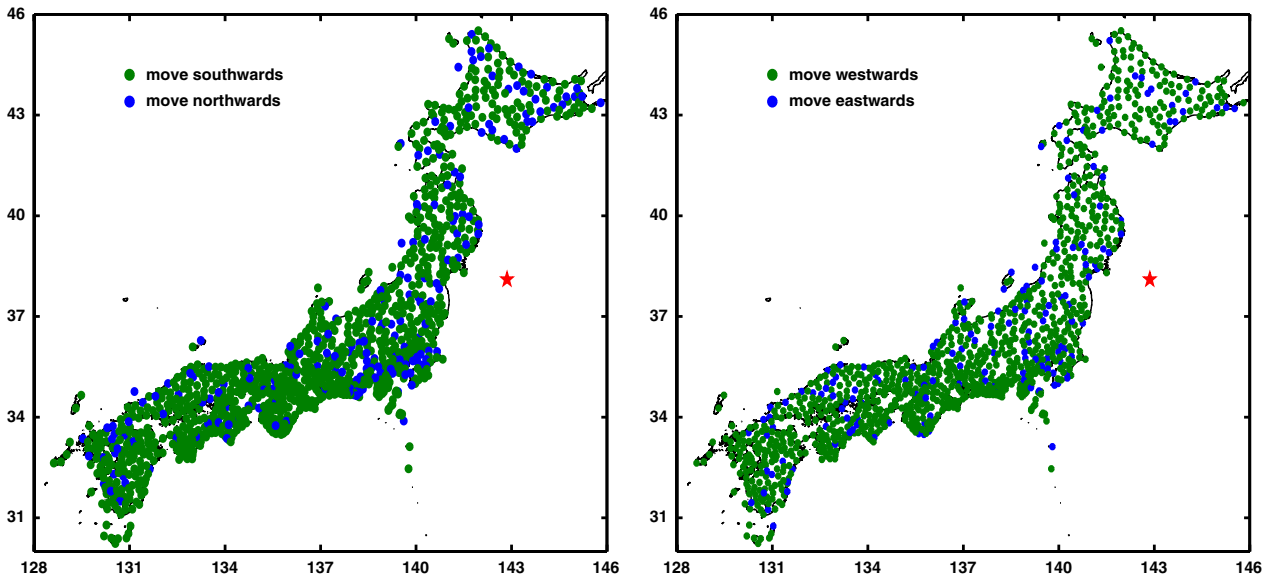

Fig. 8 The patterns of the movements of 1198 GEONET stations within 1 s: left panel—epoch between 15:01:04 and 15:01:05 with 1008 stations moving southward, and right panel—epoch between 15:03:39 and 15:03:40 with 1029 stations moving westward

15:03:40 with 80.80, 84.14 and 85.89% of the GEONET stations simultaneously moving upward, southward and westward, respectively. We choose the two epochs with the largest probabilities to show the patterns of movement within 1 s in Fig. 8. For simplicity, we only show the directions of movement in different colors without the magnitudes in Fig. 8. It can be clearly seen from Fig. 8 that both panels look green, though some blue solid circles are scattered here and there, indicating that a great majority of the GEONET stations move in the same direction within 1 s (left panel—southward; right panel—westward). Although these probabilities are very high, it may hardly be imagined that a large scale of sudden movement could occur repeatedly between 14:59:04 and 15:03:40. Together with the above seismic test, even with only a very small number of available KiK-net seismographs, the detected sudden movements after the earthquake could be unidentified artifacts of GPS data processing, though it might be possible that they be physical signals.

Physical signals or unidentified artifacts?

We have processed the 1 Hz GPS data from 1198 GEONET stations and obtained the 1 s precise point positioning (PPP) time series of positions for these stations. A quick inspection of the PPP waveforms has led us to find that 76.21% of the GEONET stations in the Japanese islands consistently move suddenly within 1 s between 14:59:45 and 14:59:46. We have also carried out different independent tests to check whether the detected sudden movement is real, namely (i) a detailed analysis of GPS measurement errors in the long and short terms; (ii) processing the high-rate GPS data of IGS stations around Japan to test whether the displacement pattern outside the Japanese islands is consistently similar in the surrounding countries; (iii) independently processing the GEONET data with another well-known GPS data processing software system GIPSY; (iv) performing a statistical hypothesis testing by assuming that any movement at the epoch is purely due to white noise and (v) comparing the GEONET results with those from borehole KiK-net strong motion seismographs. The first four tests fully support a physical signal, while the KiK-net is marginally consistent with the GEONET results. Due to problems such as tilting, rotation and baseline corrections inherent with strong motion seismographs, the KiK-net results may not be conclusive as an independent test. We cannot confirm independently from borehole KiK-net strong motion seismographs whether the detected sudden movements by GEONET are physically real or unidentified artifacts due to GPS data processing. In case that this observation of sudden movements within 1 s would be real, a physical explanation is unclear.

The last independent test has been directly applied to the GPS PPP waveforms of the 1198 GEONET stations in order to examine whether the same phenomenon occurs at other epochs. A new computer code has pinpointed that the same phenomenon of sudden movement has indeed occurred at the second epochs of 14:59:04, 15:01:04 and 15:03:39, with even a higher percentage of 80.80, 84.14 and 85.89 among the 1198 GEONET stations, respectively. These high-rate GPS PPP results

might imply that Japan seemingly moves suddenly and repeatedly, within 1 s soon after the 2011 Tohoku earthquake, with the highest data-based probability of about 0.86. Although the directions of the average sudden movements are roughly consistent with that of subduction of the Pacific plate, we are suspicious that the repeatedness of sudden movements within a few minutes after the main shock might not be physically reasonable or acceptable. From this point of view, although it is impossible to completely eliminate the possibility that the detected sudden movements may be physical signals, as senior GNSS experts, both theoretically and/or in practical GNSS data processing, we tend to think that the sudden movements detected by the high-rate GPS PPP are probably unidentified artifacts of GPS data processing.

Finally, we like to make some remarks. Although a maximum 85.89% (or equivalently 1029 stations) of the 1198 GEONET stations show a consistent trend of seemingly sudden movement at some epochs after the main shock, if the phenomenon would be attributed as some unidentified artifacts of GPS data processing, all the work in this paper should indicate that cutting-edge GNSS results should be interpreted with the greatest possible care in the geoscience community. More work is surely necessary in the future to help clarify possible or potential sources of artifacts from GNSS data processing, if what we found is indeed a GNSS-rooted artifact. One idea is to use GNSS Doppler measurements, together with GNSS code and phase measurements, to compute high-rate GNSS displacements and velocities, since they contain the information on both positions and velocities (see e.g., Hofmann-Wellenhof et al. 1992; Zhang 2007; Zhang and Guo 2013), but are not used in our GNSS data processing. Nevertheless, one may not be too optimistic at this moment, since current GNSS Doppler measurements are generally noisier (Zhang and Guo 2013; Crespi 2018, private email communication on March 6, 2018). The other idea is to further explore whether any unknown stochastic characteristics in GNSS measurements may potentially be related to the reported phenomenon.

Additional files

Additional file 1. The sudden displacements between 14:59:45 and 14:59:46 after the 2011 Tohuku Mw9.0 earthquake.

Authors' contributions

PX conceives the ideas of this manuscript, designs the experiments and tests, advises on and checks the GPS PPP data processing with PANDA, helps the data processing of the KiK-net strong motion seismographs and writes the manuscript. YS processes the GPS data to obtain the PPP waveforms, computes the KiK-net strong motion data and participates in error analysis. JL participates in the discussion of the detected sudden movement and error analysis and provides technical support with PANDA. TN processes the GPS data with the GIPSY software system for an independent test of the detected sudden movements. YS participates in the discussion of error analysis and results. JF suggests testing the stations outside Japan, participates in the discussion of the results and revises the manuscript. All authors read and approved the final manuscript.

Author details

[1] Disaster Prevention Research Institute, Kyoto University, Uji, Kyoto 611-0011, Japan. [2] College of Marine Geosciences, Ocean University of China, Qingdao, People's Republic of China. [3] GNSS Research Center, Wuhan University, Wuhan 430071, People's Republic of China. [4] School of Geomatics, Xi'an University of Science and Technology, Xi'an 710054, People's Republic of China. [5] Department of Earth and Environmental Sciences, Michigan State University, East Lansing, MI 48824, USA.

Acknowledgements

We are very much indebted to Prof. Masataka Ando for his thorough reading of the manuscript and advice on the writing, for hours of discussions and for his many constructive comments on the observed phenomenon. We thank Prof. Benjamin Fong Chao for the discussion of the observed results and Dr. Rongjiang Wang for the private communications on the KNET and KiK-net coseismic displacements. We also thank two anonymous reviewers for their constructive comments, which help restructure part of the materials presented in this paper.

Competing interests

There is no competing interest with this manuscript.

Availability of data and materials

We acknowledge the Geospatial Information Authority (GSI) of Japan for providing all the GEONET RINEX GPS raw data via Japan Association of Surveyors and the National Research Institute for Earth Science and Disaster Prevention for the KNET and KiK-net strong motion data.

Consent for publication

Not applicable.

Ethics approval and consent to participate

Not applicable.

Funding

This work is partially supported by the National Natural Science Foundation of China (41874012, 41231174 and 41674013).

Appendix: The electronic materials

Due to the limited space, we list, as an electronic file (or Additional file 1: Table S1), all the coordinate results obtained by post-processing the 1 Hz GPS data of the GEONET stations in the PPP mode with the software system PANDA. Additional file 1: Table S1 contains the three-component displacements between 14:59:45 and 14:59:46 for all the GEONET stations, with seven columns: GEONET station code numbers, the coordinates of the stations (latitude, longitude and height (meters)) and the three-component displacements of the stations between 14:59:45 and 14:59:46 (east, north, vertical) in millimeters.

Publisher's Note

Received: 14 January 2019 Accepted: 1 April 2019
Published online: 11 April 2019

References

Aoi S, Kugugi T, Fujiwara H (2004) Strong-motion seismograph network operated by NIED: K-NET and KiK-net. J Assoc Earthq Eng 4:65–74

Bassiri S, Hajj GA (1993) Higher-order ionospheric effects on the global positioning system observables and means of modeling them. Manuscr Geod 18(5):280–289

Blewitt G, Heflin MB, Hurst KJ, Jefferson DC, Webb FH, Zumberge JF (1993) Absolute far-field displacements from the 28 June 1992 Landers earthquake sequence. Nature 361:340–342

Bock H, Dach R, Jäggi A, Beutler G (2009) High-rate GPS clock corrections from CODE: support of 1 Hz applications. J Geod 83:1083–1094

Böhm J, Niell A, Tregoning P, Schuh H (2006) Global mapping function (GMF): a new empirical mapping function based on numerical weather model data. Geophys Res Lett 33:L07304

Branzanti M, Colosimo G, Crespi M, Mazzoni A (2013) GPS near-real-time coseismic displacements for the great Tohoku-oki earthquake. IEEE Geosci Rem Sens Lett 10:372–376

Brunner FK, Gu M (1991) An improved model for the dual frequency ionospheric correction of GPS observations. Manuscr Geod 16(3):205–214

Choi K (2004) Modified sidereal filtering: implications for high-rate GPS positioning. Geophys Res Lett 31:L22608

Clarke PJ, Davies RR, England PC, Parsons B, Billiris H, Paradissis D, Veis G, Cross PA, Denys PH, Ashkenazi V, Bingley R, Kahle HG, Muller MV, Briole P (1998) Crustal strain in central Greece from repeated GPS measurements in the interval 1989–1997. Geophys J Int 135:195–214

Dieterich JH (1974) Earthquake mechanisms and modeling. Ann Rev Earth Planet Sci 2:275–301

Dong D, Fang P, Bock Y, Webb F, Prawirodirdjo L, Kedar S, Jamason P (2006) Spatiotemporal filtering using principal component analysis and Karhunen–Loeve expansion approaches for regional GPS network analysis. J Geophys Res 111:B03405

Fialko Y (2006) Interseismic strain accumulation and the earthquake potential on the southern San Andreas fault system. Nature 441:968–971

Frank FC (1966) Deduction of earth strains from survey data. Bull Seismol Soc Am 56:35–42

Graizer V (2010) Strong motion recordings and residual displacements: What are we actually recording in strong motion seismology? Seismol Res Lett 81:635–639

Grapenthin R, Freymueller JT (2011) The dynamics of a seismic wave field: animation and analysis of kinematic GPS data recorded during the 2011 Tohoku-oki earthquake, Japan. Geophys Res Lett 38:L18308

Hofmann-Wellenhof B, Lichtenegger H, Collins (1992) GPS theory and practice. Springer, New York

Huang Z, Zhao D (2013) Relocating the 2011 Tohoku-oki earthquakes (M 6.0–9.0). Tectonophysics 586:35–45

Iinuma T, Hino R, Kido M, Inazu D, Osada Y, Ito Y, Ohzono M, Tsushima H, Suzuki S, Fujimoto H (2012) Coseismic slip distribution of the 2011 off the Pacific coast of Tohoku Earthquake (M9.0) refined by means of seafloor geodetic data. J Geophys Res 117:B07409

Kato T, Terada Y, Kinoshita M, Kakimoto H, Isshiki H, Matsuishi M, Yokoyama A, Tanno T (2000) Real-time observation of tsunami by RTK-GPS. Earth Planets Space 52:841–845

King RW, Masters EG, Rizos C, Stolz A, Collins J (1985) Surveying with GPS. In: Monograph 9, School of Surveying. The University of New South Wales, Australia

Kinoshita S (1998) Kyoshin net (K-NET). Seismol Res Lett 69:309–332

Kouba J (2009) A guide to using international GNSS service (IGS) products. IGS Central Bureau, Pasadena

Kouba J, Héroux P (2001) Precise point positioning using IGS orbit and clock products. GPS Solut 5(2):12–28

Larson KM (2009) GPS seismology. J Geod 83:227–233

Larson KM, Bodin P, Gomberg J (2003) Using 1-Hz GPS data to measure deformation caused by the Denali fault earthquake. Science 300:1421–1424

Larson KM, Bilich A, Axelrad P (2007) Improving the precision of high-rate GPS. J Geophys Res 112:B05422

Lay T, Kanamori H (2011) Insights from the great 2011 Japan earthquake. Phys Today 64:33–39

Li X, Ge MR, Zhang Y, Wang RJ, Xu PL, Wickert J, Schuh H (2013) New approach for earthquake/tsunami monitoring using dense GPS networks. Sci Rep 3:2682. https://doi.org/10.1038/srep02682

Liu J, Ge M (2003) PANDA software and its preliminary result of positioning and orbit determination. J Nat Sci Wuhan Univ 28:603–609

Moschas F, Stiros S (2015) Dynamic deflections of a stiff footbridge using 100-Hz GNSS and accelerometer data. J Surv Eng 141:04015003

Mood AM, Graybill FA, Boes DC (1974) Introduction to the theory of statistics, 3rd edn. McGraw-Hill, London

Prescott WH, Davis JL, Svarc JL (1989) Global positioning system measurements for crustal deformation. Science 244:1337–1340

Ragheb AE, Clarke PJ, Edwards SJ (2006) GPS sidereal filtering: coordinate-and carrier-phase-level strategies. J Geod 81(5):325–335

Reid HF (1910) The California earthquake of April 18, 1906. The mechanics of the earthquake. In: Report of the state earthquake investigation commission, vol 2. Carnegie Institution of Washington, Washington DC

Sato M, Ishikawa T, Ujihara N, Yoshida S, Fujita M, Mochizuki M, Asada A (2011) Displacement above the hypocenter of the 2011 Tohoku-Oki earthquake. Science 332:1395

Segall P (1997) New insights into old earthquakes. Nature 388:122–123

Simons M, Minson SE, Sladen A, Ortega F, Jiang JL, Owen SE, Meng LS, Ampuero JP, Wei SJ, Chu RS (2011) The 2011 magnitude 9.0 Tohoku-Oki earthquake: mosaicking the megathrust from seconds to centuries. Science 332:1421–1425

Smalley R Jr (2009) High-rate GPS: How high do we need to go? Seismol Res Lett 80:1054–1061

Shu Y, Shi Y, Xu PL, Niu X, Liu JN (2017) Error analysis of high-rate GNSS precise point positioning for seismic wave measurement. Adv Space Res 59:2691–2713

Thatcher W, Marshall G, Lisowski MJ (1997) Resolution of fault slip along the 470-km-long rupture of the great 1906 San Francisco earthquake and its implications. J Geophys Res 102:5353–5367

Thatcher W, Foulger GR, Julian BR, Svarc J, Quilty E, Bawden GW (1999) Present-day deformation across the Basin and Range province, western United States. Science 283:1714–1718

Wang R, Parolai S, Ge M, Jin M, Walter TR, Zschau J (2013) The 2011 Mw9.0 Tohoku earthquake: comparison of GPS and strong-motion data. Bull Seismol Soc Am 103:1336–1347

Wdowinski S, Bock Y, Zhang J, Fang P, Genrich J (1997) Southern California permanent GPS geodetic array: spatial filtering of daily positions for estimating coseismic and postseismic displacements induced by the 1992 Landers earthquake. J Geophys Res 102:18,057–18,070

Whitten CA, Claire CN (1961) Analysis of geodetic measurements along the San Andreas fault. Bull seism Soc Am 50:404–415

Xu PL (2005) Sign-constrained robust least squares, subjective breakdown point and the effect of weights of observations on robustness. J Geod 79:146–159

Xu PL, Shi C, Fang R, Liu JN, Niu X, Zhang Q, Yanagidani T (2013) High-rate precise point positioning (PPP) to measure seismic wave motions: an experimental comparison of GPS PPP with inertial measurement units. J Geod 87:361–372

Xu PL, Shu YM, Niu X, Liu JN, Yao WQ, Chen Q (2019) High-rate multi-GNSS attitude determination: experiments, comparisons with inertial measurement units and applications of GNSS rotational seismology to the 2011 Tohoku Mw9.0 earthquake. Meas Sci Technol 30:024003. https://doi.org/10.1088/1361-6501/aaf987

Zhang J (2007) Precise velocity and acceleration determination using a standalone GPS receiver in real time. Ph.D. Thesis, RMIT, Australia

Zhang XH, Guo BF (2013) Real-time tracking the instantaneous movement of crust during earthquake with a stand-alone GPS receiver. Chin J Geophys 56(6):1928–1936. https://doi.org/10.6038/cjg20130615 **(in Chinese)**

Zumberge J, Heflin M, Jefferson D, Watkins M, Webb F (1997) Precise point positioning for the efficient and robust analysis of GPS data from large networks. J Geophys Res 102(B3):5005–5017